Analysis of Gravity Signals and Gravity Potential Determination Using Order 8 Multiresolution Analysis Discrete Wavelets

KENNETH J. FRIESEN, NICK PANAGIOTACOPULOS
Department of Electrical Engineering,
California State University at Long Beach; Long Beach,CA 90840, USA

and
WILLIAM L. SJOGREN
Jet Propulsion Laboratory, California Institute of Technology; Pasadena,CA 91109, USA

Abstract: Our study focused upon comparing the effectiveness of the discrete wavelets in extracting gravitational data from orbital velocity signals of satellites orbiting the moon versus extracting this data by the method of least squares and polynomial approximation. The results of our study show that the multiresolutional analysis(MRA) of order 8 discrete wavelets shows promise as an alternate filtering process in converting orbital velocity signals to gravitational data for any planet under consideration. As a filter the discrete wavelets have several properties that make them a desirable choice: the property of perfect reconstruction of signals and high computational speed.

Key Words: wavelet, multiresolutional analysis (MRA), moon, gravity field, potential.

1 Introduction

One of the important products of NASA's Lunar Prospector mission to the moon was measurement of the line-of-sight(LOS) velocity obtained from Doppler radio signals sent by orbiting satellites. These velocity signals were recorded by earth based tracking stations at Goldstone (California), Madrid(Spain), and Canberra(Australia) This velocity contains information necessary to make a determination of the gravitational field of the moon. The current procedure of processing these signals is first to remove all velocity components from known sources such as the velocity due to earth's rotation, the velocity of the space craft due to orbital maneuvers, the centrifugal velocity of the space craft due to the moon's central gravity, orbital motion of the moon, and all the velocity contributions that do not have significance. This is followed by a least squares fit estimating the space craft position and velocity as well as many parameters of the gravity field leaving residual velocity that still has systematic signatures. The residual velocity is then approximated by cubic splines which removes the random noise preserving only the systematic signatures. The spline fit can then be differentiated producing acceleration profiles which represent the gravitational effects from lunar oblateness and from local surface conditions producing anomalies in the gravitational field. The goal of our research was to investigate a new approach in processing the residual velocity using order 8 MRA discrete wavelets to see if the results would be of higher resolution than those of the current method. The approach is producing a higher resolution acceleration profile of the moon's gravitational field. We begin with a description of the fundamentals of geopotential and wavelet theory followed by descriptions of both the current method and the use of wavelets in converting residual velocity to acceleration.

2 Fundamentals

Fundamental to our presentation are the gravitation model and the essentials of wavelet theory.

2.1 Gravity Potential

The gravitational potential function for all planetary bodies is

$$P(r,q,f) = GM/r[1+\sum_{n=0}^{\infty}(a_p/r)^n ... \\ ...\sum_{m=1}^{n}(C_{n,m}\cos(mq)+S_{n.m}\sin(mq))P_{n,m}(\sin j)]$$

where r is the radius from the planet center, a_p is the surface radius, θ is the longitude, φ is the latitude, G is the Universal Gravitational Constant, M is the planet mass, $C_{n,m}$ and $S_{n,m}$ are the spherical harmonic coefficients, and $P_{n,m}$ is the associated Legendre polynomial of degree n, order m. By restricting the limit of summation of the degree index to 75, this

function is said to be the potential function of degree 75 and order 75. Since a gravity surface of the moon of degree 75 , order 75 had been produced prior to the Lunar Prospector Mission, the accelerations produced from processing the residual velocity are only "refinements" of the existing 75^{th} degree, 75^{th} order gravity model. In the central region of the moon: 30°W to 30°E longitude by 30°S to 30°N latitude the predominant term in the model for gravitational effects due to oblateness and surface anomalies is the harmonic acceleration, which is the radial component of gravitational acceleration minus the term defining the planet's centrifugal gravity. The harmonic acceleration is the partial derivative of the potential function with respect to r minus the centrifugal term – GM/r^2

$$A_{r(75,75)} = GM / r^2[\sum_{n=0}^{75}(n+1)[(a_p / r)^n C_{n,0} P_{n,0}(\sin(f))...$$

$$-\sum_{m=1}^{n}(C_{n,m}\cos(mq) + S_{n,m}\sin(mq))P_{n,m}(\sin f))]$$

The first summand on the right hand side is the component of zonal harmonics known as the "J" term, and the second summand on the right hand side is the component of tesseral harmonics and is known as the " harmonics" term. In the central region refinements are produced by addition of the accelerations derived from the residual velocity to the harmonic acceleration

$$A_r(\text{refined}) = A_{r(75,75)} + \mathbf{a}$$

where **a** is either the CS acceleration or the wavelet acceleration.

2.2 Wavelet Theory

Discrete wavelets are functions that form a basis for the functional space $L^2(\Re)$, the space of all functions for which the integral of the square of its absolute value taken over the time interval $(-\infty,\infty)$. The wavelet basis for $L^2(\Re)$ actually is a dual basis consisting of a pair of basis window functions known as the scaling function and the wavelet function respectively. As window functions these functions are defined only on compact intervals; each basis can only represent the portion of a function that is defined in the window. To cover the interval $(-\infty,\infty)$, the window must be translated by an integral index **k** This functional pair partitions the space $L^2(\Re)$ into a decomposition that has a special algebraic structure, which is known as a multiresolutinal analysis decomposition (MRA) of $L^2(\Re)$. Both the scaling function, $\varphi(t)$, and the wavelet function, $\psi(t)$, generate a sequence of subspaces, $\{V_n\}$ by the scaling function, and $\{W_n\}$, by the wavelet function, whose union generates $L^2(\Re)$ as $n \to \infty$. Both functions have the special mathematical property that the bases function for each indexed subspace is the scaled version of that function scaled by the factor 2^n, V_n is generated by $\varphi(2^n t)$ and W_n is generated by $\psi(2^n t)$. The two sequences of subspaces differ however in their internal structures: The sequence $\{V_n\}$ is mutually inclusive whereas the sequence $\{W_n\}$ is mutually orthogonal.

Any signal $f(t) \in L^2(\Re)$ has two series expansions relative to the pair of wavelet bases. The first is a series expansion relative to the scaling function bases

$$f(t) = \sum_{j=-\infty}^{\infty}\sum_{k=-\infty}^{\infty} h_{j,k} f(2^j t - k)$$

The second series expansion is relative to the wavelet bases

$$f(t) = \sum_{j=-\infty}^{\infty}\sum_{k=-\infty}^{\infty} d_{j,k} y(2^j t - k)$$

where the coefficients in the wavelet series $\{\mathbf{d}_{j,k}\}$ are the called the "discrete wavelet transform" of f(t) relative to the wavelet basis $\psi(2^j t-k)$. The wavelet series expansion acts as a filter on the signal; segmenting the signal into its components in disjoint frequency bands as well into local values contained within the window interval for $\psi(2^j t-k)$, $[t-k/2^j, t+ k/2^j]$. Generation of a wavelet series expansion for the signal is the *decomposition phase* of the wavelet filtering operation. Each scaled wavelet function subdivides the spectrum $[0,\pi]$ into frequency bands decreasing by inverse powers of 2, ($(\pi/2, \pi]$, $(\pi/4, \pi/2]$, …).]. This property of the wavelet expansion comes from the orthogonality of the subspaces $\{W_n\}$. For finite signals, the range of this series expansion in the scaling index is N, where N is the exponent of 2 that equals or exceeds the number of data points and the range of each translation index is 2^j, for j <= N. The segmentation of the frequency spectrum is from $(0,\pi/2^N]$ to $(\pi/2,\pi]$. Generation of a scaling function series expansion is the *reconstruction phase* of the wavelet filtering operation, since this operation combines the disjoint segments of the signal in the wavelet series expansion into a series expansion where the bases functions are not mutually orthogonal.

2.2.2 Orbits

The orbits comprising the complete data base that we used traversed the near side of the moon from the lunar north pole to the lunar south pole in a near perpendicular plane to the lunar equator; extending from -106°W to 106°E (a longitudinal drift of only few degrees characterized each orbit as it traversed the face of the moon). With few exceptions the longitudinal offset of each of these orbital tracks was approximately 1 degree at the lunar equator. Each point in the track was defined by its altitude above the surface and by its longitude and latitude. Thus as each track passed over its respective strip of the moon's surface, it registered velocity induced by the gravity at that particular point.

3 Problem Statement

The residual velocity contains high frequency noise, originating from measurement and signal transmission, that corrupts determination of the underlying velocity profile. The noise is removed by cubic spline approximation. The one problem in this method is that no polynomial approximation procedure can extract a velocity function from discrete velocity values without approximation errors; however, as the order of approximation increases, the errors become extremely small. The precise determination of local topographical anomalies requires that all short-time perturbations in the velocity profile be retained in the approximation process regardless of how small these perturbations may be. These transient features appear as short duration "sharp peaks" or "dips" of relatively small magnitude. We present a comparative description of the current procedure and of wavelet filtering in the production of the acceleration profile from the initial LOS velocity data.

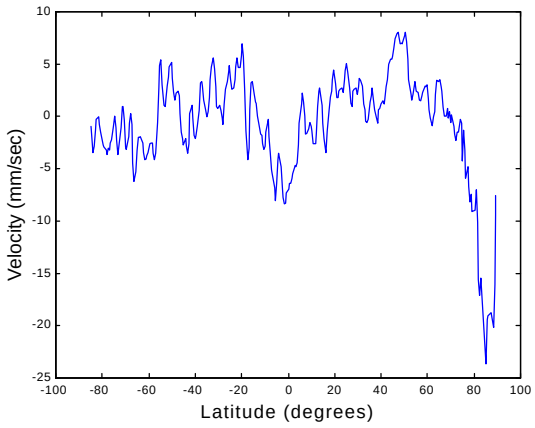

Fig. 1 Residual Velocity

3.1 Current Method of Converting Residual Velocity to Acceleration

The LOS velocity is composed of the following components, each from a distinct source of acceleration:

(1) Velocity from Newtonian point-mass acceleration. relative to the moon's center.
(2) Velocity due to oblate accelerations from the earth, sun, and nearby planets
(3) Velocity due to acceleration from radiation pressure, spacecraft control operations, and gas leaks.
(4) Velocity due to acceleration from general relativity.
(5) Velocity due to acceleration from the oblateness of the moon.

The first four of these components is removed from the LOS velocity by computation producing the residual velocity. The residual velocity contains systematic signatures and high frequency random noise. To produce the required acceleration induced by the gravitational field of the moon it is necessary to remove all random noise. This is accomplished by by a cubic spline fit. The resulting cubic spline (CS) velocity is a continuous noise free velocity profile from which the requisite acceleration can be computed by first order differentation. (See Fig 2 for CS velocity and Fig 4. for CS acceleration).

The output of this procedure is a table for each orbital track containing the following data items: (1)time that signal was transmitted from the spacecraft, (2)the residual velocity, (3)spacecraft position (altitude, longitude,latitude), (4)CS velocity, (5)CS acceleration, and, (6) harmonic acceleration. These tables for the orbital tracks of the Lunar Prospector provided us with the database for our research.

3.2 Converting Residual Velocity to Acceleration Using Wavelets

Wavelet filtering replaces least squares fit and cubic spline approximation in removing random noise from the residual velocity. Noise removal is accomplished by wavelet decomposition and partial reconstruction producing a noise free velocity profile from which an acceleration profile can be produced by differentation.

3.2. Signal Decomposition and Reconstruction

We performed a complete order 8 MRA decomposition of the residual velocity from each orbital track. Since each track contained 700-800 data points an order 8 wavelet filter produces 8 decomposition levels (level 2 was the lowest decomposition level and level 10 was

the highest decomposition level). We then reconstructed the signals first to level 5 , level 6, and level 7 respectively. Examination of randomly selected samples of levels 8 through 10 reconstructed signals revealed in each case that these signals contained too much of the high frequency noise to be acceptable candidates for computing acceleration. We made careful comparisons of the level 5 and level 6 reconstructed signals to a selected sample of CS velocities. If a particular level of reconstructed velocity was to be accepted for a particular orbit it must be in good correspondence to the CS velocity over the relatively smooth regions, deviating only from the CS velocity by small perturbations of sharp peaks or dips. In this effort we found that level 5 reconstructions were overly smooth and did not show good correspondence. Level 6 reconstructions showed very good correspondence to the selected sample of CS velocities over all smooth areas, deviating only by small perturbations. Level 7 reconstructions compared as favorably to some of the selected samples but not in every case. Therefore, we chose to compute our wavelet based accelerations from level 6 reconstructions in all the cases.

3.3 Acceleration

Since our level 6 reconstructed residual velocities existed as discrete data sets rather than as a continuous velocity , the only way in which we could convert these signals to acceleration was to use first order differences divided by the intervening time interval. We faced the initial problem of excessive numerical error if we simply divided the sequential velocity points by the intervening time interval in seconds. The magnitude of the velocity signals were in the range of 0.1 and 10 mm/sec while the average time interval is 5.0 seconds. Since discrete wavelets converge to a continuous wavelet function we can justify using the discrete first order approximation to the actual derivative as a means of computing the derivative if the time interval is sufficiently small. To overcome the problem of convergence we chose to scale the time interval in minutes rather than in seconds (5.0 seconds ≈ 0.08min). Thus we computed the acceleration in $m/(min^2)$ initially and the converted this to $m/(sec^2)$ by dividing by 60. To validate this method, we applied it to the CS velocity and compared the results to the CS acceleration; obtaining perfect agreement in each case.

4 Results

We made an extensive analysis of both the resultant velocity and the computed acceleration to determine the validity of our initial hypothesis.

4.1 Velocity Analysis

In comparing the processed residual velocities and the corresponding accelerations we selected a sample orbit: The orbit traced a vertical path crossing the lunar equator at 2 degrees west longitude. Figure 2 contains a plot of the CS velocity, and Figure 3 contains a plot of the MRA level 6 (L6) reconstructed velocity. Comparing the two figures one sees noticeable differences in the range of –60 deg to –20 deg latitude where the L6 velocity is more definitive. The lobes at 0 deg and 50 deg latitude in both figures is nearly identical; however, the lobes in the level 6 velocity have more slightly “jagged” edges due to small perturbations. As we said in the preceding sections the sections the reconstructed velocity must correspond to the CS velocity in all smooth regions; differing only in small intervals where the reconstructed velocity shows deviations more clearly.

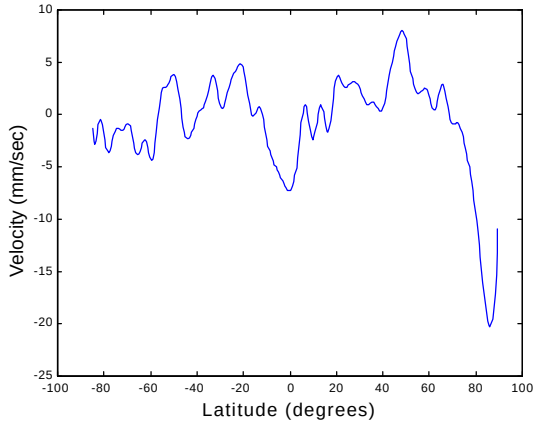

Fig. 2 Cubic Spline Velocity

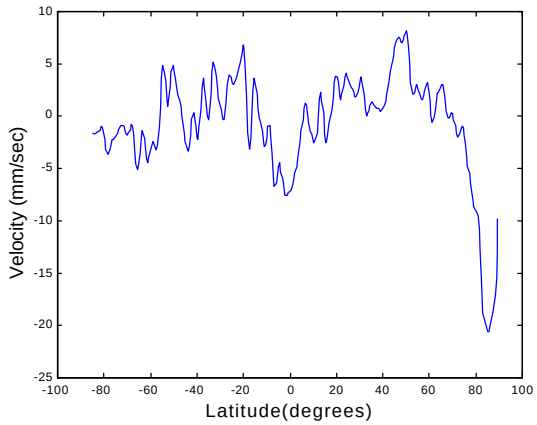

Fig. 3 L6 Velocity

4.2 Acceleration Analysis

Figures 4 and 5 contain plots of the CS acceleration and the wavelet L6 acceleration. The unit of acceleration used by NASA is the milligal(mgal), 1 milligal = 10^{-2}mm/sec^2. The differences between the two velocities shows up as more pronounced differences in the two accelerations. In the range of –60 deg to –20 deg latitude where the L6 velocity showed grater definitiveness, the L 6 acceleration has noticeably grater magnitude and sharper oscillations than does the CS acceleration. In the remaining regions the two accelerations are of similar magnitude but the L6 acceleration shows sharper oscillations which is due to the many more small perturbations of the L6 velocity.

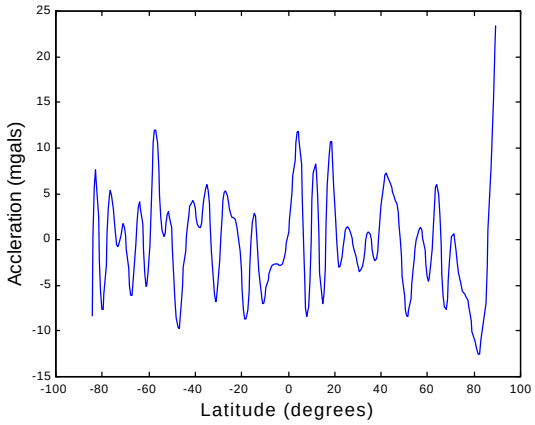

Fig.4 Cubic Spline Acceleration

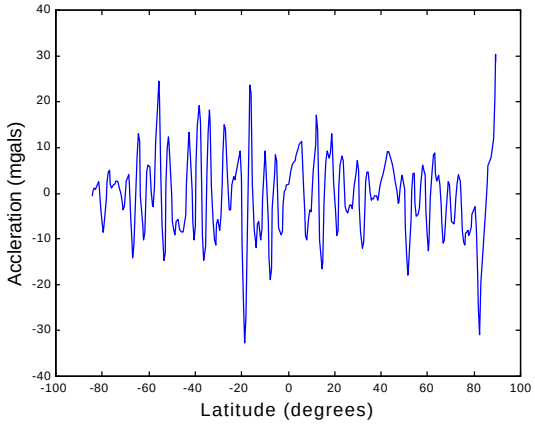

Fig. 5 L6 Acceleration

Most important in acceleration analysis is the comparison between the refinements to the radial acceleration of the 75th degree, 75th order produced from the CS acceleration and the L6 acceleration. Figures 6 and 7 contain acceleration surfaces of the refined radial acceleration produced from the L6 acceleration and the CS acceleration respectively. Our illustrative orbit track (2°W) passes through two prominent craters: Ptolemaeus (2°W,8°S) and Alphonsus(3°W,14°S); and the two refined accelerations should show local differences in major craters. Figs 6 and 7 are gravity surfaces in the region 10°W to 0° longitude and -15°S to -5°S latitude for the CS refined acceleration and the wavelet L6 refined acceleration. Comparison of the two acceleration profiles shows that the L6 acceleration has a steeper gradient reaching a greater local maximum and a lesser local minimum in the regions of these two craters than does the CS acceleration. In the region of the crater Ptolemaeus , the L6 refined acceleration has two low contour levels: -50 mgal and – 40mgal; whereas the CS refined acceleration shows no contour lines at all in this region. In the region of Alphonsus, the L6 refined acceleration shows an elongated contour of –40mgal containing a depression at –50 mgal. The CS refined acceleration shows a similar elongated contour only at – 40 mgal that is actually west of the locale of Alpohonsus, and the enclosed area is smaller. This is evidence of the lower level refined accelerations produced by the wavelet L6 acceleration.

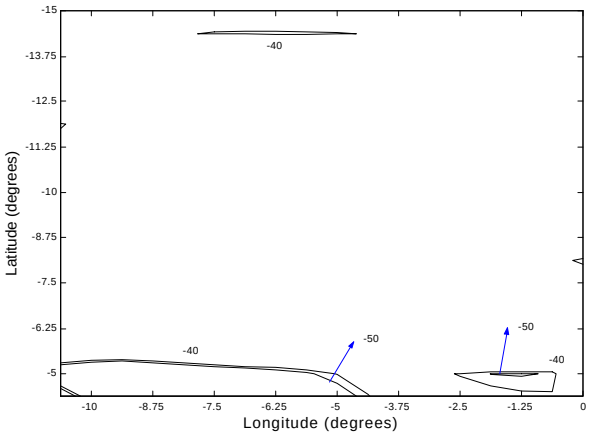

Fig 6. Gravity Map CS Acceleration

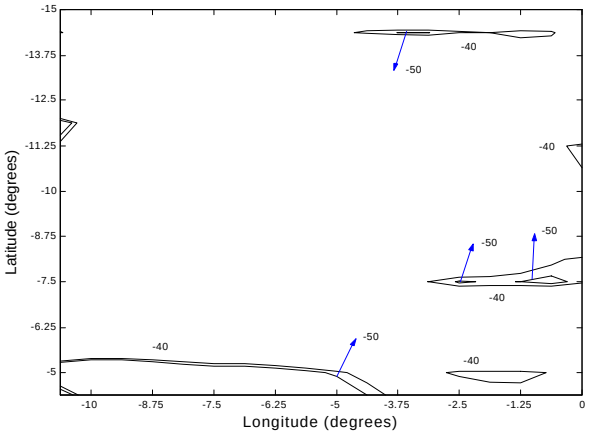

Fig. 7 Gravity Map L6 Acceleration

5 Conclusion

Careful examination of Fig's 1, 2, and 3 will show that the L6 velocity better preserves many of the signatures of the residual velocity than does the CS velocity. Due to the higher resolution of the L6 velocity, the L6 acceleration has greater magnitude and frequency. When added to the harmonic acceleration, the L6 acceleration produces a local gravity map that reveals a steeper gradient in regions with significant surface anomalies: the two significant acceleration troughs at the sites of the craters Ptolemaeus and Alphonsus give evidence of this. We had to concentrate our velocity and acceleration analysis on a single orbit track, but the differences between the L6 velocity and the CS velocity and the resulting two accelerations are typical for all remaining orbits; in some cases they are slightly less pronounced in other cases they are slightly more pronounced. Examination of this and other cases shows that the use of MRA order 8 discrete wavelets does produce higher resolution residual velocity and as a consequence higher resolution acceleration.

References

[1] *Mathematical Formulation of the Double-Precision Orbit Determination Program, Technical Report 32-1527; T*heodore J. Meyer*;* Jet Propulsion Laboratory, Pasadena, CA; 1971.

[2] *Improved Gravity Field of the Moon from Lunar Prospector*; A.S. Konopliv, et all: Science, vol 281, Sept. 1998.

[3] P.M. Mueller and W.L. Sjogren; Science, 161, 680, 1968.

Acknowledgements

We would like to thank Dr. Alexander Konopliv, Jet Prolusion Laboratory, for providing the data and for technical support and Prof Courtney Coleman, Harvey Mudd College, for suggestions in mathematical model development